MgO/Fe(001) and MgO/Fe(001)-$p(1\times1)$O interfaces for magnetic tunnel junctions: A comparative study

A. Cattoni, D. Petti, S. Brivio, M. Cantoni, R. Bertacco, and F. Ciccacci
L-NESS, Dipartimento di Fisica, Politecnico di Milano, via Anzani 42, 22100 Como, Italy
(Received 23 December 2008; revised manuscript received 7 August 2009; published 29 September 2009)

The chemical, structural, and electronic properties of MgO/Fe(001) and MgO/Fe(001)-$p(1\times1)$O interfaces for magnetic tunnel junctions (MTJs) have been widely investigated by means of electron spectroscopy. In particular, we present a detailed analysis of the spin-resolved electronic structure above the Fermi level, carried out by spin-polarized inverse photoemission and absorbed current spectroscopy. The MgO barrier presents good crystallinity and sharp interfaces when grown both onto Fe(001) and Fe(001)-$p(1\times1)$O. Moreover, we find that the exchange splitting of unoccupied bands is essentially the same for the two MgO/Fe interfaces, even though it is different for the two starting surfaces, being larger in Fe(001)-$p(1\times1)$O than in Fe(001). Our findings indicate that Fe(001)-$p(1\times1)$O is a good candidate for the realization of heterostructures for magnetic tunnel junctions because of its high chemical stability and reproducibility, as compared to clean Fe(001).

DOI: 10.1103/PhysRevB.80.104437 PACS number(s): 75.70.Cn, 85.75.−d, 79.60.−i

I. INTRODUCTION

Magnetic tunnel junctions (MTJs) based on MgO(001) barriers and ferromagnetic (FM) electrodes represent a very popular and widely investigated subject in the field of spintronics. Since the pioneering theoretical predictions[1,2] of a symmetry filtering effect in Fe/MgO/Fe(001) heterostructures giving rise to tunneling magnetoresistance (TMR) values on the order of 1000%, much work has been done in order to find experimental evidence of this effect. In 2004, two papers[3,4] announced TMR values of 180% and 220%, respectively, at room temperature (RT) in Fe/MgO/Fe(001) MTJs grown by molecular-beam epitaxy (MBE) and CoFe/MgO/CoFe MTJs grown by sputtering. Since then, much work has been done on MTJs based on MgO(001) barriers in order to find the best combination of ferromagnetic electrodes giving the highest TMR together with relatively small bias dependence and reasonable resistance area product. TMR values at room temperature as high as 600% have been recently announced,[5] as a result of the optimization of the interface quality and the choice of CoFeB as electrode. The high magnetoresistive response, together with the stability and reliability of these devices, make them very attractive for applications in data storage[6] and magnetic sensors.[7]

However, some fundamental aspects of these MTJs remain unclear such as the role of B in CoFeB electrodes and the impact of the interfacial oxidation at the FM/MgO interface. It is widely accepted that interfaces play a major role in determining the final performances of MTJs, as it has been demonstrated that the insertion of ultrathin layers in between the FM and the MgO barrier completely alters the performance of the junction.[8] In particular, the interfacial oxidation of the FM due to MgO growth has been widely investigated in view of the possible deterioration of the TMR induced by the FeO_x interfacial layer. Zhang *et al.*[9] calculated the effect of different oxidation conditions in the FeO_x layer, with x varying from 0 to 1, finding a rapid decrease in the conductance ratio between the two spin channels when x increases in asymmetric junctions FeO_x/MgO/Fe(001). Tusche *et al.*[10] presented the calculated TMR for asymmetric junctions (Fe/MgO/FeO) and symmetric junctions (FeO/MgO/FeO) involving fully oxidized FeO layers, and predicted non-negligible negative TMR values [−74% with six monolayers (ML) of MgO] for asymmetric junctions, at variance with the very high positive TMR values for symmetric junctions (5750% with six ML of MgO). Heiliger *et al.*[11] consider symmetric and asymmetric junctions; their calculations indicate a sizable reduction in the TMR in the symmetric case with respect to the ideal case without oxidation, while for the asymmetric state a high value of the TMR is predicted for one polarity of the applied bias. This overview clearly demonstrates that the role of the interface oxidation in determining the TMR is not fully understood and, in particular, that it is not completely clear if oxidation in itself really reduces the TMR. On the other hand, it has been demonstrated by spin-polarized electron spectroscopy[12–14] that the surface spin-dependent effects (namely, exchange splitting and spin asymmetry in absorbed current spectroscopy) of the Fe(001) surface are greatly enhanced upon a particular oxygen exposure treatment giving rise to the well-known[12,13,15–17] Fe(001)-$p(1\times1)$O structure, corresponding to one ML of oxygen adsorbed onto the Fe(001) surface. The large exchange splitting and the high order and stability of the Fe(001)-$p(1\times1)$O surface are appealing features in view of the fabrication of MTJs with high TMR, as spin filtering is essentially ensured by symmetry filtering, which strongly depends on the interface quality. In this scenario we carried out a detailed comparative study of the MgO/Fe(001) and MgO/Fe(001)-$p(1\times1)$O interfaces looking at the interface chemistry, crystallinity, and spin-dependent electronic properties. We investigated structures with MgO thickness ranging from 2 to 9 ML, i.e., from the initial stage of formation of the interface to a typical thickness of the barrier in a MTJ, with great attention also to the quality of the MgO barrier, which plays a major role in determining the ultimate TMR. Much work has been done on the occupied electronic states of the MgO/FM interface, essentially via photoemission spectroscopy (PES) with spin polarization,[18,19] while here we focus on the unoccupied states, investigated by spin-polarized inverse photoemission (SPIPE) and absorbed cur-

rent spectroscopy (ACS). Unoccupied states close to the Fermi level clearly participate in the tunneling process at nonzero bias, so that their investigation provides useful information on the electronic structure, complementary to those obtained by photoemission.

Additional information on the chemical and structural properties of the interfaces have been obtained by x-ray photoemission spectroscopy (XPS) and low-energy electron diffraction (LEED), respectively. The picture arising as a whole from our detailed analysis is that the MgO/Fe(001)-$p(1\times1)$O interface is a good candidate for the realization of MTJs based on MgO epitaxial barriers, essentially because it has the same interfacial spin-dependent electronic structure as MgO/Fe(001), while the Fe(001)-$p(1\times1)$O surface shows higher chemical stability and reproducibility.

II. EXPERIMENT

The heterostructures have been grown and analyzed *in situ* in an ultrahigh vacuum system equipped with a MBE apparatus and a chamber for electron spectroscopy, as described in detail elsewhere.[20]

Clean and well-ordered Fe(001) surfaces were prepared by depositing a thick Fe film (1000 Å) on commercial MgO(001) substrates as described elsewhere.[21] The Fe(001)-$p(1\times1)$O surface was obtained by an exposure to 30 L of molecular oxygen (1 L$=10^{-6}$ Torr s) and flash heating at 900 K of a clean Fe(001) surface.[13]

MgO was deposited at RT and at a slow rate of ~0.2 Å/min by evaporation of pieces of stoichiometric MgO contained in a Ta crucible and heated by electron bombardment. The coverage was estimated by a quartz microbalance and then checked by XPS to ensure high reproducibility for the thickness of the MgO layers deposited on the two surfaces considered in this work. We investigated MgO layers with thicknesses ranging from 2 to 9 ML (1 ML corresponding to 2.1 Å), as grown and after two annealing treatments: A1 (15 min at 570 K) and A2 (flash heating up to 870 K).

During SPIPE and ACS, samples are magnetized in plane along the [100] direction of the Fe lattice (i.e., the [110] direction of the MgO lattice due to the lattice rotation which minimizes the mismatch), with the spectra taken in remanence, as usual in electron spectroscopy. A collimated and transversely polarized electron beam with 25% polarization impinges on the sample, and then the ACS spectra are recorded by measuring the absorbed current running to the ground. The SPIPE spectra are taken in the isochromat mode by collecting photons at a fixed photon energy, $h\nu=9.3$ eV, while varying the incident-beam energy.[22] Data are collected at RT and at normal incidence, thus probing states along the ΓH line in the bcc Brillouin zone (BZ).

III. RESULTS AND DISCUSSION

A. Structural and chemical properties

Qualitative information on interfacial structural order for different MgO coverage and after annealing treatments has been obtained by LEED. In Fig. 1, we report the corresponding LEED patterns. Panels (a) and (b) refer to 2 ML of MgO deposited at RT onto clean Fe(001) and Fe(001)-$p(1\times1)$O, respectively. The two images have been recorded at 190 and 180 eV in order to maximize the contrast for each sample, and it is evident that a high contrast and spot sharpness is obtained in both cases. This indicates the good crystallinity of ultrathin MgO films grown onto the Fe(001)-$p(1\times1)$O surface, arising from the high order of the chemisorbed $p(1\times1)$ oxygen. The increase in the MgO coverage onto both surfaces still gives an ordered overlayer for deposition at RT, as shown in panel (c) for the case of Fe(001)-$p(1\times1)$O covered by four ML of MgO. The A1 treatment clearly improves the film crystallinity and increases the coherence length for LEED, thus resulting in sharper spots, as shown in panel (d). Additional annealing (A2 treatment) results in a further improvement of crystallinity, manifested in a slight sharpening of the LEED spots (data not shown). Note that at nine ML of MgO, i.e., for a thickness of MgO suitable for the realization of MTJs with high TMR, satellite spots appear around the main diffraction spots for both interfaces.[23] They reflect the formation of misfit dislocations without evident dependence on the state of oxidation of the Fe substrate. To summarize, LEED reveals that MgO grows on Fe(001)-$p(1\times1)$O with essentially the same crystallinity observed for MgO/Fe(001).

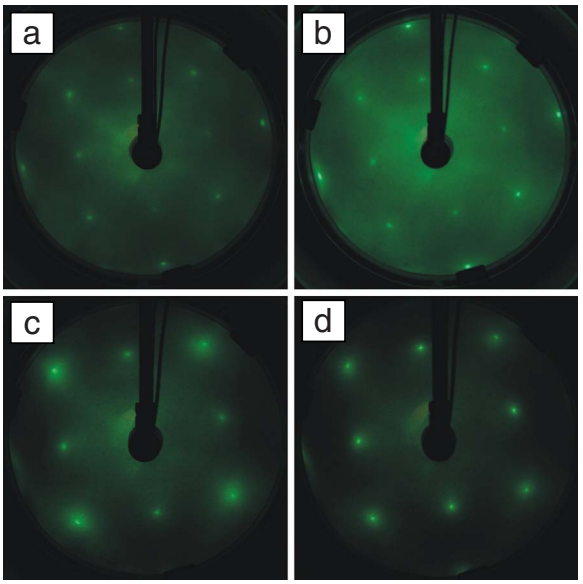

FIG. 1. (Color online) LEED pattern taken on (a) 2 ML of MgO on Fe(001), (b) 2 ML of MgO on Fe(001)-$p(1\times1)$O, (c) 4 ML of MgO on Fe(001)-$p(1\times1)$O grown at RT, and (d) 4 ML of MgO on Fe(001)-$p(1\times1)$O after annealing A1 at 570 K.

We consider now the impact of the MgO deposition on the interface chemistry and, in particular, on the Fe oxidation state, as seen by XPS. In Fig. 2, we plot the Fe2p spectra taken with a standard Mg-Kα x-ray source ($h\nu=1253.6$ eV, the signal from the α_3 and α_4 satellites was carefully subtracted), from MgO films with different thicknesses grown either on clean Fe(001) (upper panel) or Fe(001)-$p(1\times1)$O (lower panel). The spectra have been collected at 60° emission angle with respect to the sample normal in order to

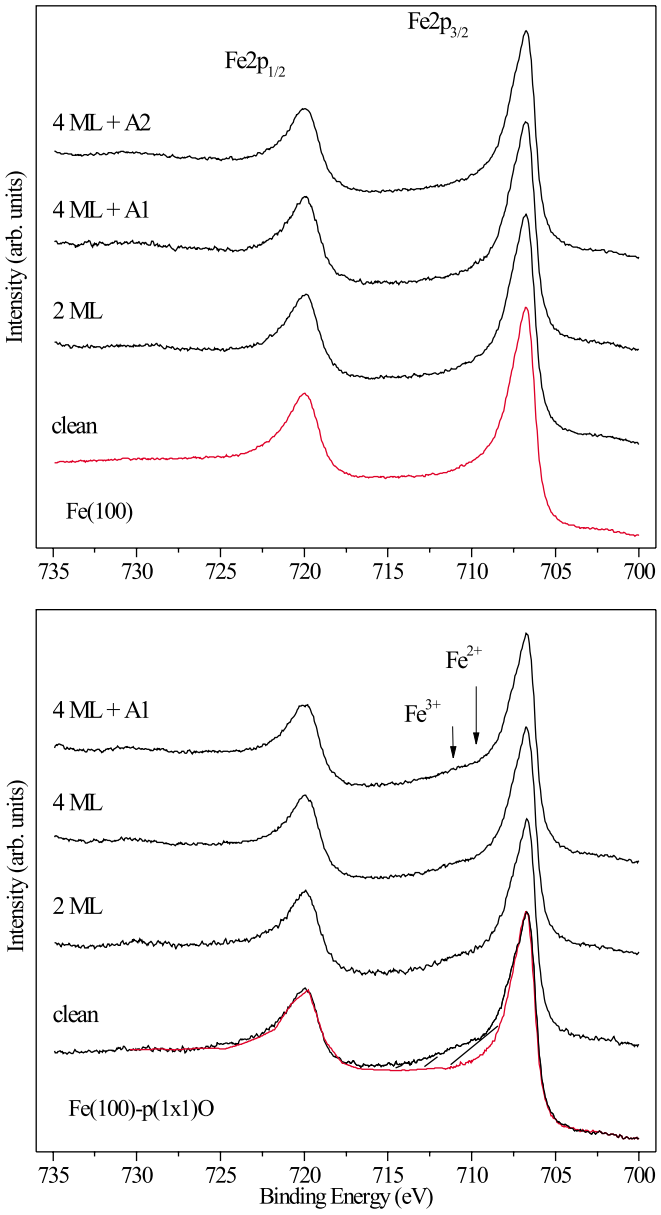

FIG. 2. (Color online) Fe2p XPS spectra taken at 60° of collection angle and at different MgO coverage on Fe(001) (upper panel) and Fe(001)-$p(1\times1)$O (lower panel). A1 and A2 indicate different annealing treatments (see text). The hatched area represents the contribution of Fe atoms interacting with O to the spectrum from Fe(001)-$p(1\times1)$O.

increase the surface interface sensitivity. In consideration of the standard curve for inelastic mean-free path, the use of a laboratory Mg source to excite Fe2p levels implies a probing depth of about 13 Å. In our case, however, working at a large collection angle (60°), such values are reduced by a factor of 2, considerably increasing the surface sensitivity. In the case of clean Fe(001) (upper panel) the spectra essentially consist of a doublet at the proper binding energy of metallic Fe (706.7 eV for Fe $2p_{3/2}$). Deposition of MgO, even though followed by annealing (either the A1 or A2 treatment), does not produce any spectral variation: all the curves in the stack in the upper panel of Fig. 2 can be superposed, within the experimental error. We conclude that a negligible Fe-O interaction takes place at the interface and this behavior is stable up to 870 K. The sensitivity of this analysis can be deduced from the comparison with the spectrum referring to the Fe(001)-$p(1\times1)$O substrate (lower panel, bottom spectrum). In this case, in fact, an additional signal on the high-binding-energy side of both the Fe $2p_{3/2}$ and Fe $2p_{1/2}$ peaks is clearly visible, at the energies expected for Fe^{2+} and Fe^{3+} ions arising from Fe atoms interacting with O (at 711.1 and 709.7 eV, respectively, shown by vertical arrows in Fig. 2).[24] The signal coming from the interfacial Fe-O layer is indicated by the hatched area in Fig. 2 (bottom panel), which represents the additional contribution to the spectrum when it is fitted with the line shape of the spectrum from clean Fe(001) (red curve). From the weight of this component relative to that from pure metallic Fe, the thickness of the resulting interfacial Fe-O layer can be estimated to be roughly 1.5 Å. This is coherent with the already established presence of one ML of oxygen at the Fe(001)-$p(1\times1)$O surface.[12,13,15,16] By comparing these results with the XPS spectra from MgO/Fe(001) samples, we can estimate the degree of Fe-O interface interaction taking place when depositing MgO on clean Fe(001). In fact, our XPS analysis is based on the chemical shift of the Fe2p peak, which in turn depends on the charge transfer from Fe toward O. The absence of any line-shape variation (in the upper panel of Fig. 2) points toward a much smaller interaction than in Fe(001)-$p(1\times1)$O. By taking into account the experimental uncertainties, we can set an upper limit of some 10% of ML for the interfacial Fe-O layer formed in MgO/Fe(001) systems. This result is in good agreement with synchrotron-radiation photoemission data[19] on MgO/Fe(001) interface prepared in similar conditions, with a photon energy allowing higher surface sensitivity with respect to laboratory XPS. The authors of Ref. 19 found no evidence at all of the formation of an interfacial Fe-O layer in the MgO/Fe(001) system. A very limited degree of oxidation has been also reported by Miyokawa *et al.*[25] for sharp MgO/Fe(001) interfaces investigated by XAS. A larger degree of oxidation has instead been reported by Tusche *et al.*,[10] who found an $FeO_{0.5}$ interfacial layer in MgO/Fe(001) studied by surface sensitive diffraction. Such a small quantitative discrepancy may be explained by slightly different preparation procedures, as it is well known that O excess during MgO growth plays an important role in the final oxidation.[26] In any case, all data point toward a much smaller Fe-O interaction in MgO/Fe(001) interface than on the Fe(001)-$p(1\times1)$O surface, where Fe atoms in the top layer are in strong interaction with one full ML of chemisorbed oxygen. This is also in agreement with the first-principles calculations, which show a negligible charge transfer between Fe and O atoms at sharp Fe/MgO interfaces.[9]

The case of MgO growth on Fe(001)-$p(1\times1)$O is very similar, notwithstanding the initial presence of an Fe-O surface layer: we find no significant increase upon MgO deposition of the corresponding XPS signal. The Fe2p line shape remains stable even after annealing at 870 K of four ML of MgO (Fig. 2, lower panel). The initial conditions are thus preserved during the barrier growth onto the FM.

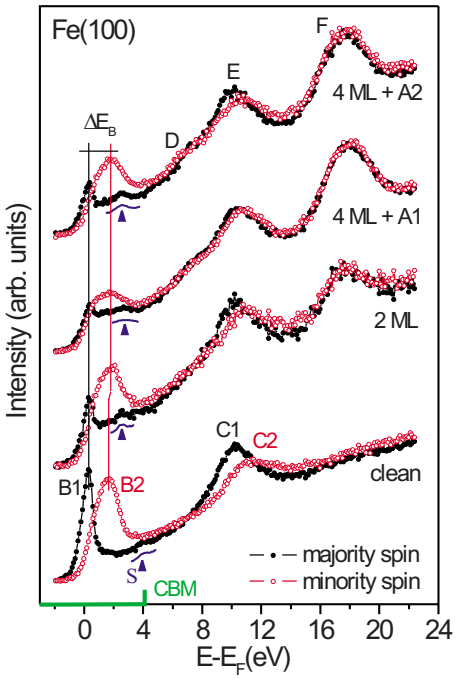

FIG. 3. (Color online) SPIPE data for different MgO coverage on Fe(001). The position of the MgO gap is indicated on the energy scale with a thick green line. The blue curves are the result of a smoothing of the majority spectrum in the region of the image state(s), whose position is marked with a triangle.

The similarity of the two systems holds true for the electronic structure as well, as shown by spin-polarized data discussed below.

B. Spin-polarized electronic structure

The study of the spin-polarized electronic structure above the Fermi level has been carried out by SPIPE. In Fig. 3, we report the spin-polarized spectra from the Fe(001) surface with different MgO coverage: 0, 2, 4 ML. For the 4 ML case we also considered the effect of A1 and A2 annealing treatments. Due to dipole selection rules and due to the fact that electrons impinging on the sample at normal incidence have Δ_1 symmetry, only Δ_1 and Δ_5 final states are allowed in the transition occurring during the inverse photoemission process.[27] However, at the fixed photon energy of our detector (9.3 eV), there is no direct transition connecting Δ_1 initial states to Δ_1 final states close to the Fermi level in the bulk Fe band structure, so that Δ_1 states relevant for tunneling cannot be probed by SPIPE. Instead, close to the Fermi level the spectrum of clean Fe (Fig. 3, bottom) is dominated by two peaks, B1 and B2, with majority and minority spin characters, respectively, reflecting transitions into Δ_5 final states close to the H'_{25} point of the BZ.[12,27] These states belong to the Δ_5 band crossing the Fermi level and are then involved in the tunneling process, according to the scheme of symmetry filtering proposed by Butler *et al.*[1,2] They participate in conduction in both spin channels but with a lower transmission probability with respect to Δ_1 states, so that a big difference in the conductance between the parallel and antiparallel states is observed. In particular, the energy separation (ΔE_B) between B1 and B2 is related to the exchange splitting of Δ_5 bands close to the H point.[12] At higher energy another doublet C1-C2 appears, corresponding to transitions into final states close to H'_{15}, whose energy separation (ΔE_C) reflects the exchange splitting in this particular point of the BZ. Another feature S is visible in the spectrum [at ~3.8 eV in the spectrum for clean Fe(001)], marked with a blue triangle, which originates from transitions into the image state resonance, where electrons are confined between the energy barrier at the sample surface and the image potential produced by the electron approaching the Fe surface.[28] MgO deposition attenuates the Fe features, not changing, however, the overall structure of the corresponding spectrum, and causes the appearance of new MgO derived peaks. The onset of the latter contribution is given by the MgO conduction-band minimum, which, on the basis of the position of the MgO valence-band maximum (determined by ultraviolet photoemission spectroscopy data, not shown) and of its energy gap of 7.8 eV, is placed at 4.4 eV above the Fermi level (vertical green thick line in Fig. 3). Three MgO features (labeled as D, E, and F) can be identified, as seen more easily in the spectra from relatively thick MgO films (see below); they can be found at 6.9, 10.5, and 17.6 eV, respectively, and their intensities increase with the MgO coverage. No energy dispersion with MgO coverage has been detected. Moreover, they are completely unpolarized, not presenting any dependence on the electron spin. In comparison with the calculated band structure of MgO,[29] we find that D arises from a transition to a final state close to the Γ point, while E and F are connected to final states close to the X point of the BZ.

The image state S, being predominantly located outside the solid, is heavily affected by MgO deposition and it indeed shifts by 1.4 eV toward lower energies already for 2 ML coverage (see. Fig. 3). This shift is mainly connected to the decrease in the surface work function (WF) as the image states are bounded to the vacuum level. The deposition of MgO is expected to produce a reduction in the work function due to the presence of electropositive Mg atoms, which create a surface dipole, lowering the surface energy barrier. The growth of MgO, however, could also cause the change in the reflection coefficient of the wave functions at the solid surface, as it essentially depends on the surface band structure, with possible modifications of the image state position. In any case, the MgO gap coincides with the energy range of image states, so that their existence is still allowed after MgO deposition, and the influence of the change in the reflection coefficient turns out to be lower than that of the work function. To prove the connection between the change in the energy of the image states and the work function we measured the latter by ACS (data not shown), looking at the edge of the absorption of the incident electron beam.[30] Starting from the Fe(001) work function of 4.75 eV, for 2 ML of MgO we found a sizable reduction down to 3.40 eV, with a decrease of 1.35 eV, which is in close agreement with the shift of the image state (1.40 eV) within the experimental accuracy (see Table I). After the initial shift, minor variations are observed when increasing the MgO coverage or after annealing (Fig. 3, topmost spectra), with relatively small changes in the image state energy, which follow the trend of work-function changes.

TABLE I. Exchange splitting of feature B (ΔE_B), energy position of the image state (E_S), and WF for different MgO coverage and annealing onto the Fe(001) and Fe(001)-$p(1\times1)$O surfaces. The change in the image state position (ΔE_S) and WF (Δ_{WF}) relative to the clean surface are also reported.

MgO coverage	ΔE_B (eV)	E_S (eV)	WF (eV)	ΔE_S (eV)	ΔWF (eV)
Fe(001)	1.35 ± 0.05	3.95 ± 0.05	4.75 ± 0.05		
2 ML	1.50 ± 0.05	2.55 ± 0.05	3.40 ± 0.05	1.40	1.35
4 ML+A1	1.45 ± 0.05	2.65 ± 0.10	3.40 ± 0.05	1.30	1.35
4 ML+A2	1.50 ± 0.05	2.40 ± 0.05	3.15 ± 0.05	1.55	1.65
Fe(001)-$p(1\times1)$O	1.55 ± 0.05	4.05 ± 0.05	4.50 ± 0.05		
2 ML	1.50 ± 0.05	2.70 ± 0.05	3.40 ± 0.05	1.35	1.10
4 ML+A1	1.60 ± 0.05	3.00 ± 0.10	3.95 ± 0.05	1.05	0.55
9 ML+A1	1.50 ± 0.10		3.60 ± 0.05		0.90

We consider next in detail the Fe contribution, which is only minimally altered by the MgO overlayer,[31] but contains the spin-dependent information that is most interesting for MTJ applications. Looking at the evolution of the exchange splitting of peaks B and C we find an increase in ΔE_B from 1.35 ± 0.05 to 1.50 ± 0.05 eV upon MgO deposition, accompanied by a decrease in ΔE_C from 0.90 to 0.55 eV.[32] The latter result is heavily influenced by the presence in the region of the doublet C of the intense unpolarized MgO peak E, which causes an apparent reduction in the splitting ΔE_C. The doublet B, instead, lies in the gap of the MgO, and in turn does not suffer from any masking effect from the MgO overlayer, which makes the measured increase in ΔE_B fully reliable. MgO deposition on the clean surface, thus, leads to an Fe exchange splitting very similar to that present in Fe(001)-$p(1\times1)$O ($\Delta E_B=1.55$ eV, see Table I). This occurs at a very small MgO coverage and then remains stable, indicating the persistence of a ferromagnetic interfacial layer, with larger spin-dependent effects than in the clean surface. Annealing essentially produces an increase in the surface order, reflected by a sharpening of B1, B2, and S which is clearly visible, especially when comparing spectra taken on four ML of MgO/Fe(001) after A1 and A2 annealing. Increasing the annealing temperature from 570 to 870 K produces a sizable effect in the spectra, while minor improvements in the sharpness of Fe peaks are observed when comparing the spectra taken on four ML of MgO before (data not shown) and after A1 annealing. On the contrary, the exchange splitting and the energy position of the various peaks are practically unchanged after annealing, as reported in Table I, where the results from SPIPE and ACS data on clean Fe(001) and Fe(001)-$p(1\times1)$O are summarized.

Let us consider now the case of the growth of MgO onto the Fe(001)-$p(1\times1)$O surface. In Fig. 4, we report the spectra from the free Fe(001)-$p(1\times1)$O surface, along with those corresponding to 2, 4, and 9 ML of MgO. For four and nine ML, spectra after A1 annealing are reported. The spectrum from the free surface presents essentially the same structure as that taken on clean Fe(001) but with a sizable increase in the exchange splitting of peaks B and C, which are now 1.55 and 1.05 eV, respectively, to be compared with 1.35 and 0.90 eV in the case of the clean Fe(001) surface (see Table I). The spectral evolution upon MgO deposition strictly follows that was discussed for the case of the clean Fe(001) substrate. In this case, the most relevant quantity, i.e., the exchange splitting ΔE_B, which is not affected by MgO-derived states, stays stable at 1.55 ± 0.05 eV also after the deposition of four ML and the A1 annealing, while its value can be hardly evaluated in the case of nine ML coverage, where in any case a sizable splitting is present. The image state S presents an evolution, which is again very similar to that observed in the case of the clean Fe surface,

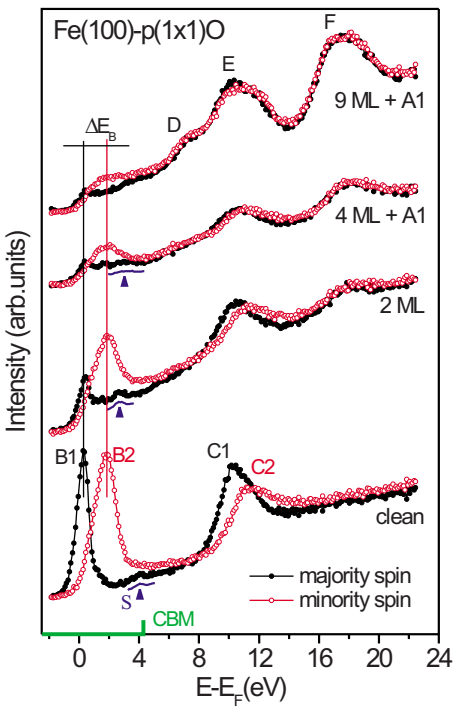

FIG. 4. (Color online) SPIPE data for different MgO coverage and annealing treatments on Fe(001)-$p(1\times1)$O. The position of the MgO gap is indicated on the energy scale with a thick green line. The blue curves are the result of a smoothing of the majority spectrum in the region of the image state(s), whose position is marked with a triangle.

with a shift to lower energy coherent with the overall reduction in the work function (see Table I). The strong oscillations in the work function, which have already been observed by Wu *et al.*,[33] only partially influence the position of the image state, possibly indicating compensation by the variation in the reflection coefficients due to the surface modifications upon deposition and annealing.

Our results show that the initial exchange splitting of Fe(001)-$p(1\times1)$O is maintained upon MgO deposition while it is increased in the case of the growth onto Fe(001): this is indeed the major difference in the trend of ΔE_B for MgO growth onto the two templates The asymptotic situation, however, is more or less the same: at four ML coverage essentially the same ΔE_B value [1.50 ± 0.05 eV for MgO/Fe(001)] and [1.60 ± 0.05 eV for MgO/Fe(001)-$p(1\times1)$O] is found. This finding is in close agreement with the results of Ref. 33, showing that the asymmetry of the electron reflectivity at 14 ML of MgO is essentially the same for the growth onto both templates. In fact, the asymmetry essentially reflects the spin-polarized electronic structure at the interface and gives information very similar to that provided by SPIPE.

Finally, following theoretical[17] and experimental[14] results on Fe(001)-$p(1\times1)$O, we can ascribe the exchange splitting increase in the MgO/Fe interface to the corresponding increase in the interface Fe magnetic moment. This can in turn be related to charge and structural rearrangements occurring upon MgO deposition on Fe(001), similar to those taking place at the Fe(001)-$p(1\times1)$O surface due to O chemisorption. Structural rearrangements and chemical interactions between Fe and O atoms occur in parallel and it is very hard to clearly separate them. However, since our XPS data show that the Fe-O interactions are different in the two cases, while the spin-dependent electronic structure is the same, we suggest that the dominant role is played by structural rearrangement, i.e., by the change in the Fe-Fe interlayer distance. An increase in such interlayer distance has been indeed reported for the MgO/Fe(001) interface,[9] similar to that measured[15] and calculated[17] for the Fe(001)-$p(1\times1)$O surface. On the other hand, it has to be noted that calculations of the equilibrium structure for a chemically sharp MgO/Fe interface predict a decrease rather than an increase in the Fe-Fe spacing at the interface.[34] However, also in this case the authors find an increase in the interfacial Fe magnetic moment with respect to the bulk. This represents an additional indication of a strong influence of the structure on interfacial magnetism in MgO/Fe interface.

To summarize, our analysis indicates that controlled growth of MgO onto clean Fe does not reduce the interface exchange splitting, which is instead enhanced. On the other hand, our measurements demonstrate that similar or better results in terms of the interfacial exchange splitting can be achieved also starting from a well-controlled oxygen exposure, i.e., that giving rise to Fe(001)-$p(1\times1)$O.

IV. CONCLUSIONS

We have carefully investigated the formation of the MgO barrier onto the clean Fe(001) and Fe(001)-$p(1\times1)$O surfaces. The picture arising as a whole is that the MgO barrier grows on both templates with high crystallinity, as seen by LEED. Concerning chemistry, we found that both interfaces are stable under annealing at up to 870 K, with a Fe-O interaction lower in the MgO/Fe(001) interface than in the MgO/Fe(001)-$p(1\times1)$O interface. SPIPE data reveal that the surface exchange splitting of Fe(001) is increased upon MgO growth, toward that of Fe(001)-$p(1\times1)$O, while being stable in the case of the Fe(001)-$p(1\times1)$O template. These findings point toward a major role of interfacial structural rearrangements occurring upon MgO deposition, instead of Fe-O interactions, in determining the surface exchange splitting. The Fe(001)-$p(1\times1)$O surface is then a good candidate for the realization of good interfaces in Fe/MgO/Fe MTJs, also considering that Fe(001)-$p(1\times1)$O presents very high chemical stability and its preparation is much easier than that of clean and well-ordered Fe(001).

As a final comment, during this work we knew that another group from the University of Nancy had obtained good results with MTJs employing Fe(001)-$p(1\times1)$O electrodes, i.e., TMR on the order of 120% with only a slight reduction with respect to the value found in optimized junctions with clean Fe electrodes annealed at the same temperature (140%).[35] This is a further confirmation of the potential of the MgO/Fe(001)-$p(1\times1)$O interface for application in magnetic tunnel junctions.

ACKNOWLEDGMENTS

This work was partially funded by Fondazione Cariplo via the project SpinBioMed (Project No. 2008.2330). The authors thank D. Chrastina for fruitful discussions and M. Leone for his skilful technical support.

[1] W. H. Butler, X.-G. Zhang, T. C. Schulthess, and J. M. MacLaren, Phys. Rev. B **63**, 054416 (2001).
[2] J. Mathon and A. Umerski, Phys. Rev. B **63**, 220403 (2001).
[3] S. Yuasa, T. Nagahama, A. Fukushima, Y. Suzuki, and K. Ando, Nature Mater. **3**, 868 (2004).
[4] S. S. P. Parkin, C. Kaiser, A. Panchula, P. M. Rice, B. Hughes, M. Samant, and S.-H. Yang, Nature Mater. **3**, 862 (2004).
[5] S. Ikeda, J. Hayakawa, Y. Ashizawa, Y. M. Lee, K. Miura, H. Hasegawa, M. Tsunoda, F. Matsukura, and H. Ohno, Appl. Phys. Lett. **93**, 082508 (2008).
[6] S. A. Wolf, D. D. Awschalom, R. A. Buhrman, J. M. Daughton, S. von Molnar, M. L. Roukes, A. Y. Chtchelkanova, and D. M. Treger, Science **294**, 1488 (2001).
[7] F. A. Cardoso, J. Germano, R. Ferreira, S. Cardoso, V. C. Martins, P. P. Freitas, M. S. Piedade, and L. Sousa, J. Appl. Phys. **103**, 07A310 (2008).
[8] J. S. Moodera, J. Nowak, L. R. Kinder, P. M. Tedrow, R. J. M. van de Veerdonk, B. A. Smits, M. van Kampen, H. J. M.

Swagten, and W. J. M. de Jonge, Phys. Rev. Lett. **83**, 3029 (1999); P. LeClair, J. T. Kohlhepp, H. J. M. Swagten, and W. J. M. de Jonge, *ibid.* **86**, 1066 (2001); F. Greullet, C. Tiusan, F. Montaigne, M. Hehn, D. Halley, O. Bengone, M. Bowen, and W. Weber, *ibid.* **99**, 187202 (2007).

[9] X. G. Zhang, W. H. Butler, and A. Bandyopadhyay, Phys. Rev. B **68**, 092402 (2003).

[10] C. Tusche, H. L. Meyerheim, N. Jedrecy, G. Renaud, A. Ernst, J. Henk, P. Bruno, and J. Kirschner, Phys. Rev. Lett. **95**, 176101 (2005).

[11] C. Heiliger, P. Zahn, B. Y. Yavorsky, and I. Mertig, Phys. Rev. B **73**, 214441 (2006).

[12] R. Bertacco and F. Ciccacci, Phys. Rev. B **59**, 4207 (1999).

[13] R. Bertacco, M. Merano, and F. Ciccacci, Appl. Phys. Lett. **72**, 2050 (1998).

[14] F. Bisio, R. Moroni, M. Canepa, L. Mattera, R. Bertacco, and F. Ciccacci, Phys. Rev. Lett. **83**, 4868 (1999).

[15] K. O. Legg, F. Jona, D. W. Jepsen, and P. M. Marcus, Phys. Rev. B **16**, 5271 (1977).

[16] J. B. Benziger and R. Madix, J. Electron Spectrosc. Relat. Phenom. **20**, 281 (1980).

[17] S. R. Chubb and W. E. Pickett, Phys. Rev. Lett. **58**, 1248 (1987).

[18] M. Sicot, S. Andrieu, P. Turban, Y. Fagot-Revurat, H. Cercellier, A. Tagliaferri, C. De Nadai, N. B. Brookes, F. Bertran, and F. Fortuna, Phys. Rev. B **68**, 184406 (2003).

[19] L. Plucinski, Y. Zhao, B. Sinkovic, and E. Vescovo, Phys. Rev. B **75**, 214411 (2007).

[20] R. Bertacco, M. Cantoni, M. Riva, A. Tagliaferri, and F. Ciccacci, Appl. Surf. Sci. **252**, 1754 (2005).

[21] R. Bertacco, S. De Rossi, and F. Ciccacci, J. Vac. Sci. Technol. A **16**, 2277 (1998).

[22] M. Cantoni and R. Bertacco, Rev. Sci. Instrum. **75**, 2387 (2004).

[23] M. Klaua, D. Ullmann, J. Barthel, W. Wulfhekel, J. Kirschner, R. Urban, T. L. Monchesky, A. Enders, J. F. Cochran, and B. Heinrich, Phys. Rev. B **64**, 134411 (2001).

[24] T.-C. Lin, G. Seshadri, and J. A. Kelber, Appl. Surf. Sci. **119**, 83 (1997).

[25] K. Miyokawa, S. Saito, T. Katayama, T. Saito, T. Kamino, K. Hanashima, Y. Suzuki, K. Mamiya, T. Koide, and S. Yuasa, Jpn. J. Appl. Phys., Part 2 **44**, L9 (2005).

[26] J. L. Vassent, A. Marty, B. Gilles, and C. Chatillon, J. Cryst. Growth **219**, 434 (2000).

[27] A. Santoni and F. J. Himpsel, Phys. Rev. B **43**, 1305 (1991).

[28] S. De Rossi, F. Ciccacci, and S. Crampin, Phys. Rev. Lett. **77**, 908 (1996).

[29] T. Kotani and H. Akai, Phys. Rev. B **54**, 16502 (1996).

[30] Electrons cannot enter the solid until their energies are higher than the vacuum level and this furnishes a simple way for measuring the work function, provided that the energy of the beam has been carefully calibrated (see Ref. 12).

[31] Actually the peak B1 is more attenuated by the MgO film than for the rest of the spectruism, but this is a well-known result explained in terms of the high sensitivity of this peak to the surface order, which is altered after MgO deposition, see also Refs. 11 and 20.

[32] Note that the value of ΔE_C is much higher than that previously reported by some of the authors in Ref. 11 from the clean Fe(001) surface, but the same holds true also for the Fe(001)-$p(1\times1)$O surface. This is probably due to the higher surface order of the samples investigated in the present paper and to some differences in the experimental apparatus.

[33] Y. Z. Wu, A. K. Schmid, and Z. Q. Qiu, Phys. Rev. Lett. **97**, 217205 (2006).

[34] B. D. Yu and J.-S. Kim, Phys. Rev. B **73**, 125408 (2006).

[35] F. Bonell, S. Andrieu, A. M. Bataille, C. Tiusan, and G. Lengaigne, Phys. Rev. B **79**, 224405 (2009).